Comparison of Commercial and Open-Source FEM Software: A Case Study

Zaheer Minhaj, Lindh Pia, Aarniovuori Lassi, Pyrhönen Juha

DOI: 10.1109/TIA.2020.3015827

Comparison of Commercial and Open-Source FEM Software: A Case Study

M. Zaheer, P. Lindh, *SM, IEEE*, L. Aarniovuori, *SM, IEEE,* J. Pyrhönen, *SM, IEEE*

LUT University
Lappeenranta, Finland

***Abstract*— 5 kW high-efficiency induction motor is analyzed using 2D open-source platform and the results are compared with commercial software and measurements. The importance of equivalent circuit parameters in 2D analyses is highlighted. The non-commercial and commercial software give similar results. The motor is further analysed in the 2.5D domain and the results are compared with measured results. The losses obtained with 2D, 2.5D and using the IEC segregation procedure of losses procedure are compared. The performance of an induction machine depends significantly on different parameters such as air gap and stator tooth tip height. Their impact on losses is studied with open-source FEA. The benefit of this open-source platform in the electrical motor analysis is the ability to use parallel-computing effectively and reduce the time required to solve the electromagnetic problem. Other benefits are the transparency of all features of the software and license-free usage. It is concluded that in 2D analyses, the open-source software can be used on industrial-scale problems as it showed acceptable results for losses, and lower computational time when using appropriate mortar and conforming boundary conditions.**

***Index Terms*-- electrical machine, finite element analysis, finite element method, induction machine, IEC-loss components, iron losses, rotor joule losses, stator joule losses.**

I. Introduction

The primary target of this research work is to benchmark a multi-physical open-source platform against well-known commercial FEA software to assess whether the open-source platform can be reliably used in electrical machine computations. Current, slip, electromagnetic torque and associated losses are calculated using the open-source platform and then compared with the results found with a commercial finite element method and measured data of a real motor. There are several reasons to favour the open-source platform. Firstly, the platform enables flexible modification of the modelling features. Secondly, it is possible to include attributes that do not exist in commercial software, for example, the open-source platform supports alternatives for pre-processing and post-processing. Lastly, use of the open-source platform permits cost-efficient massive computation [1]. Additionally, the open-source software is transparent; it is thus possible to check the source code, investigate the functionalities implemented, and judge their reliability [1]. Due to the significant license costs of commercial FEA - software, industries and research institutes are moving towards open-source or in-house software for electromagnetic analysis. Scientific research has made possible to develop various open-source libraries and FEA solvers. One of the most widely used finite element analysis software is 'FEMM' [2] that works on a MATLAB interface known as 'xfemm' [3]. However, FEMM has a substantial limitation as it does not support transient analysis. An alternative software is getDP [4], which is having its own scripting language but not emphasizing much on magnetics [5]. A MATLAB based open-source FEA library SMEKlib is capable of peforming rotating electrical machines analysis. The library uses gwrap [5] for meshing purpose. Additionally, SMEKlib is more towards on features and analysis tools but, rather focusing on user interface. Furthermore, Pyleecan (Python Library for Electrical Engineering Computational Analysis) project is aiming to provide a user-friendly, unified, and license-free Python Object-Oriented computational tool for the designs and optimization of electrical drives [6].

Traditionally, electrical machines are modelled with 2D models in FEM to get faster results. In a 2D model, however, it is not possible to consider, e.g., skewing, and if it is not considered, the model will yield unrealistic results because of elevated slot harmonics [7]. The invention of the multi-slice model (2.5D) has solved this issue to a great extent. The first model of machine multi-slicing emerged about two decades ago and subsequent development has enabled such models to approach the accuracy of 3D calculation. The 2.5D approach is less complex than 3D modelling and performs accurate skew modelling using very limited computational resources. Commercial and open-source FEM software have special built-in features for multi-slice modelling of electrical machines [8].

The open-source finite element method (FEM) utilized in this study was developed by the Finnish company CSC – IT Center for Science Ltd. Both the commercial and open-source FEM software use Maxwell's equations and the Bertotti model [9] to solve electromagnetic problems and analyse iron losses [10].

For inter-process communication and parallel processing, the open-source software utilizes the standardized message passing interface (MPI), which makes it possible to run analyses in multi-core as well as in multi-processor environments [11]. Commercial programs have also MPI, but computation with all cores of the computer is usually

M. Zaheer, P. M. Lindh, L. Aarniovuori and J. J. Pyrhönen are with LUT University, LUT School of Energy Systems, PO Box 53851, Lappeenranta, Finland

(e-mails:minhaj.zaheer@lut.fi pia.lindh@lut.fi, lassi.aarniovuori@lut.fi and juha.pyrhonen@lut.fi).

impossible. The core limit of the commercial FEA software depends on the computer used, in this case the analysis is performed with a desktop that has 12 cores, but the commercial software can only utilize 6 of them. The superior benefit of open source FEA -software is, that it can use as many cores as any desktop or supercomputer can offer. In case of Elmer nowadays 672 cores can be used. Therefore, open source FEA–software performs computations much faster than commercial ones.

An induction motor was chosen as a test case because of the widespread use of such motors in the industrial sector. They are easy to design, can work with different control principles, and operate safely within a wide field-weakening range [12]. Induction motors have often been named the workhorses of the industry, and they are widely used in variable-speed applications such as for powering conveyor belts, robots, electrical vehicles, cranes, elevators and home appliances [13]. The 5 kW motor in this work is operated with a frequency converter and is specially designed to power industrial lifting equipment.

The target of this research is analyse the energy efficiency and performance of a converter-fed machine over wide operational area. This kind of analysis with PWM supply requires an extensive number of operation points with short time step to include the high frequency harmonic content of the PWM in the solution. In the first part of the research, an alternative software package - open source platform – is tested and reported here. The design and main parameters of 5 kW prototype IM are introduced in section II. In Section III it is illustrated that with the same parameters, initial conditions and with the same input voltage, the open source software gives similar results than the well-known commercial software. The usability of the open source platform in a converter-driven machine energy efficiency analysis is further investigated in Section IV. The comparison to commercial software and to IEC loss measurements is performed in four operation points with the constant voltage-frequency ratio and different fundamental frequencies to emulate converter operation. The object is to find out if the loss results are comparable with a sinusoidal supply and in the next phase of research is PWM supply and study the harmonic losses. The computation time of the FEA is analyzed in Section V. The effect of calculation parameters on the motor loss analysis is discussed in Section VI and the last section concludes the paper.

II. Motor Design and Parameters

A model is as good as the parameters defining it. Both 2D and 3D phenomena occur in electrical machines. In 2D analyses, part of the 3D effects can be included in the solution by using analytical methods. The 5 kW motor studied in this work is a 4-pole squirrel-cage machine. Because of symmetry, it is sufficient to analyse one pole in the FEM. One fourth of the FEA model of the machine is shown in Fig. 1. The motor has 40 aluminium rotor bars and 48 stator slots. The main data of the 5 kW IM rated values are given in Table I. The motor is designed for lifting purposes and operates mainly at 75% torque. To deliberately increase the share of iron losses and better facilitate the examination of the iron losses, M800-65A material steel sheets with high specific loss value of 8 W/kg at 50 Hz are used in the construction of the rotor and stator stacks. The dimensions of the machine, stator circuit configuration and details of the winding configuration can be found in [14,15]. The rotor bars have an 8.5 degrees skew, so the magnetic flux is non-isotropic in the axial direction, and

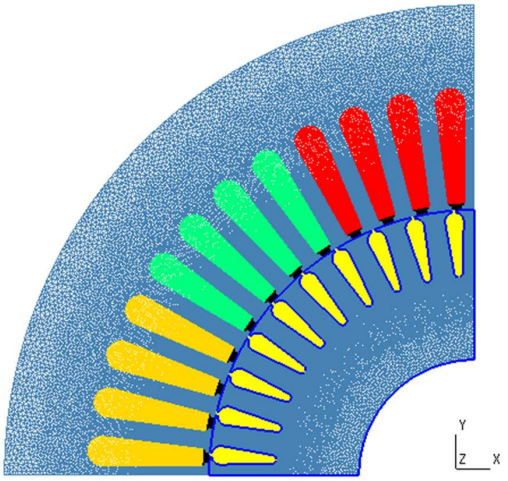

Fig. 1. One fourth of the 5 kW induction machine 2D geometry. The prototype induction motor used in this study has 48 stator slots and 40 rotor slots.

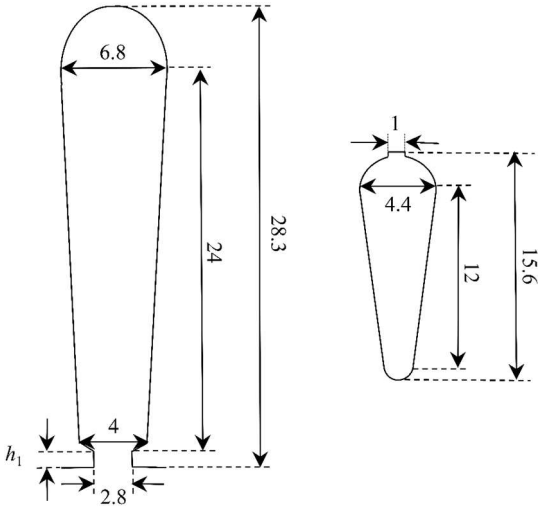

Fig. 2. Stator slot and rotor bar dimensions in millimetres. The tooth tip height h_1 = 0.7 mm.

TABLE I. Induction Machine Main Dimensions and Rated Values

Parameter	***Value***
Stator stack length, l	160 mm
Stator core external diameter, D_{se}	220 mm
Stator core inner diameter, D_s	125 mm
Air gap, δ	0.5 mm
Number of winding turns in one phase, N_s	128
Winding configuration	Y
Rated voltage, U	400 V
Rated frequency, f	50 Hz
Rated speed, n	1467 min^{-1}
Rated current, I	10.4 A

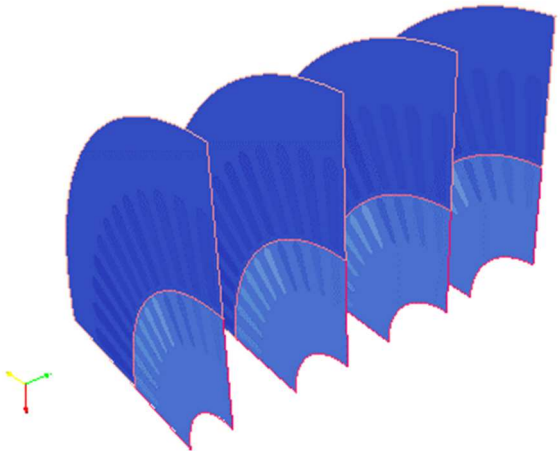

Fig. 3. One fourth of the 5kW induction machine in 2.5D geometry.

some differences to measured values are to be expected with 2D analysis.

The conductivity of aluminium and copper are 24 MS/m and 48 MS/m, respectively, when there is rated temperature rise in the winding. The stator slot and rotor bar dimensions are shown in Fig. 2.

The multi-slice model of the 5 kW induction machine has four slices and the distance between the slices is kept at 0.04 mm, Fig. 3. In the multi-slice skew model, the slices are coupled by electrical circuit variables making the model suitable for parallelization.

In the design of induction motors, equivalent circuit parameters are indispensable information, and they can be obtained analytically or by FEA [10]. The circuit parameters utilized in our research were calculated analytically. The 2D-model cannot take the three-dimensional effects into account and, therefore, they are included in an external circuit model. The motor end effects are divided into stator end-winding inductance and rotor end ring resistance and inductance [16]. The rotor circuit parameters influence the slip and related torque production of IMs.

In [17] the impedance of a machine was computed using both 2D and 3D computation and studied the effect of the end ring on machine performance. The research found that the computation results for an induction machine are very sensitive to the end ring parameters. In this study, measured phase resistance information is used in the FEA, and the resistance value is corrected to the corresponding winding temperature at the operating point studied.

A. End ring resistance

The end ring resistance is given by [18],[19]

$$R_{\text{ring}} = \frac{2\pi D_{\text{r,o}} \rho K_{\text{ring}}}{h_{\text{ring}}(D_{\text{r,o}} - D_{\text{r,i}})} \tag{1}$$

where h_{ring} represents the height of the ring, $D_{\text{r,o}}$ is the rotor outer diameter, $D_{\text{r,i}}$ is the end ring internal diameter, K_{ring} = 1.05 is a correction factor and ρ is the resistivity of the end ring conductor [18]. At high rotor frequencies the skin effect can be considered in (1) by varying the useful height of the rotor bar and the end-ring thickness. In some cases, the current does not penetrate completely into the bar (height), and therefore, the resistance should be computed for a larger diameter using a corrected rotor bar height and end-ring thickness [20].

B. End ring leakage inductance

End ring leakage inductance is given by [18]

$$L_{\text{ring}} = \mu_0 \frac{Q_{\text{r}}}{2m_{\text{s}}p}\left[\frac{2}{3}(l_{\text{bar}} - l'_{\text{r}}) + \upsilon\frac{\pi D'_{\text{r}}}{2\,p}\right] \tag{2}$$

where μ_0 is the vacuum permeability, Q_{r} is the number of rotor slots, m_{s} is the number of stator phases, p represents the number of pole pairs, l_{bar} is the rotor bar length, l'_{r} is the rotor core length, factor υ = 0.18, and D'_{r} is the average diameter of the short-circuit ring.

C. End winding leakage inductance

When applying transient 2D finite element tools, the main interest in the stator leakage components lies in the end-winding leakage connected to the FEA circuit model. Also, analytical calculation of the leakage fluxes is challenging because of the complex multilayered end-winding areas. The end-winding leakage inductance is normally given by [21].

$$L_{\text{w}} = \frac{4m}{Q_{\text{s}}} qN^2 \mu_0 l_{\text{w}} \lambda_{\text{w}} \tag{3}$$

where Q_{s} is the number of stator slots, N is the number of coil turns in series in the phase winding, l_{w} is the average end winding length. λ_{w} is a permeance factor, whose product is given as

$$l_{\text{w}}\lambda_{\text{w}} = 2l_{\text{ew}}\lambda_{\text{lew}} + W_{\text{ew}}\lambda_{\text{Wew}} \tag{4}$$

where l_{ew} is the axial length of the end winding measured from the end of the stack, and W_{ew} is the coil span. The permeance factor λ_{lew} = 0.5 and λ_{wew} is 0.2 for a three-phase two-layer stator winding and rotor cage winding type [20]. The IM circuit parameters (1)-(4) are given in Table II.

D. Iron losses

Much research has concentrated on loss studies in three-phase induction motors. Based on a 2D FEM solution, the segregation [22] of iron losses into eddy, hysteresis and excess losses. An approach [23] introduced to estimate induction motor iron and copper losses by finite element analysis considering stator winding end effects, rotor end ring effects and the skewing of rotor bars. In the open-source FEA in this study, steady-state iron losses estimation is done using the Steinmetz equation and a Bertotti model in which the total iron losses are described as a contribution of hysteresis, eddy current and excess losses [14],[24].

$$P_{\text{Fe}} = \Sigma P_k = C_1 \hat{f}_k^{a1} \hat{B}_k^{b1} + C_2 \hat{f}_k^{a2} \hat{B}_k^{b2} + C_3 \hat{f}_k^{a3} \hat{B}_k^{b3} \tag{5}$$

TABLE II. INDUCTION MACHINE PARAMETERS

Parameters			
R_s [Ω]	L_W [mH]	R_{ring} [μΩ]	L_{ring} [nH]
0.582	6	1.4	44

where P_k is a harmonic power loss component associated with the k^{th} flux density harmonic, $\hat{B}_k$ is the peak flux density value of the k^{th} B harmonic, and f_k is the k^{th} harmonic frequency [14]. The values of parameters a, b and C are obtained from curve fitting of the measured data for various frequencies and flux densities. In this research, the values for harmonic loss frequency exponents $a1, a2,$ and $a3$ are 1.0, 2.0, and 1.5. Harmonic loss field exponents $b1$, $b2,$ and $b3$ are 1.776, 2.0 and 1.5, respectively [14]. The first, second and third terms in (5) represent hysteresis, eddy current and excess losses respectively.

III. COMMERCIAL VS. NON-COMMERCIAL

The commercial FEA software also supports parallel computing but the computation time of the commercial FEA computations depends on the number of cores selected and the RAM of the operating machine [25]. For the open-source system, there is no pre-requisite to have an efficiently operating machine because it can utilize supercomputing resources and access CSC servers for robust results.

The open-source FEM uses mesh generation tools for complex geometries [26]. Importing the mesh from GMSH (open-source software) to open-source FEM could result in some dislocations of mesh nodes, which would affect the accuracy of the results. The error in the import process can be analyzed by performing root mean square error of the position of nodes deviation in x - and y–axis, in this case they are in the range of 10^{-23} and thus negligible in this context. In [26], where open-source meshing tools such as OpenFOAM, SALOME and GMSH were studied to analyze their computational meshing capabilities, it was concluded that open-source tools are less user-friendly, as there is complexity in different tool interactions and data incompatibility in various process phases [27]. In the open-source software simulations, the free CAD tool GMSH (open-source software) is used for modelling. GMSH has excellent meshing capabilities for 2D problems, because of its efficient meshing algorithms. Scripting can be done for effective construction of geometry.

Commercial tools are generally based on integrated modelling and the in-built advanced meshing capability of commercial FEA software allows it to calculate more precise results as a result of the absence of dislocations in the mesh nodes.

To check the model, verifying computations were performed in the Altair 2019 finite element program and in the open-source FEM program Elmer to acquire the waveforms at the rated load (time-stepping computation with sinusoidal voltage supply). The FEA model had 120,000 nodes and a time step of 50 μs. Torque waveforms as a function of time for both software are illustrated in Fig. 4. Torque waveform time scale is 5 ms because the fundamental waveform period is 20 ms and, because of symmetry one fourth of the supplying sine wave is taken into account. The torque ripple is large because

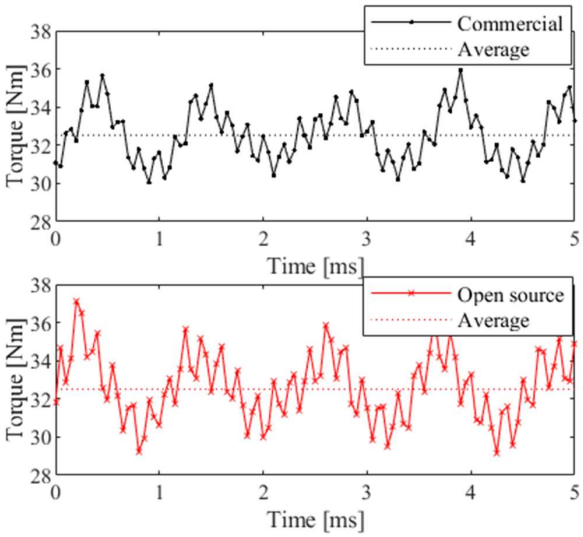

Fig. 4. Open-source and commercial FEA electric torque waveform as a function of time at 50 Hz during one fourth of a fundamental supply.

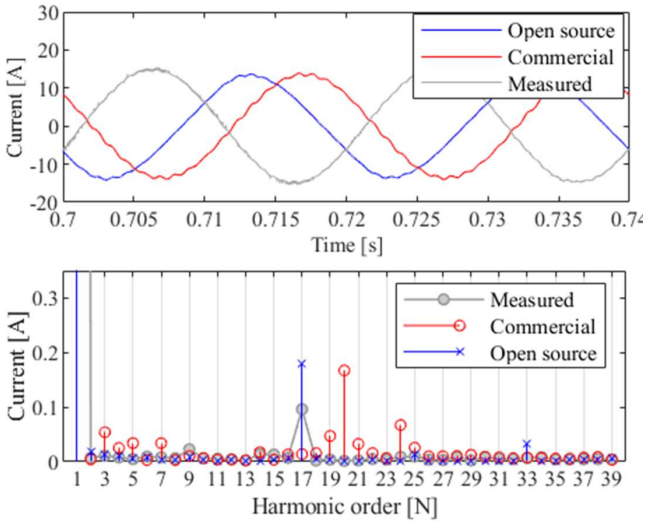

Fig. 5. Current spectra comparison at 50 Hz. Open-source, commercial FEA and measured results have been analyzed with fast Fourier transform (FFT).

rotor skewing is not considered in this 2D model [14].The measurement setup contained a 5 kW test machine, a larger IM operated with a line converter for mechanical load, instruments for measuring and recording data a generator for variable frequency and amplitude supply. The electric quantities, including voltage and current waveforms were measured with Yokogawa PX8000 power analyzer. PX8000 was equipped with Hitec Zero-Flux CURACC current measuring system (100 A-Peak). Winding resistance and Pt-100 sensors were measured with Keithley Integra Series 2701 Ethernet multimeter systems. HBM T12 digital torque measurement system with rated torque of 100 Nm was used for measuring the mechanical torque and operating speed. All measurement data were gathered with a LabVIEW™ interface on a PC. The current simulated waveform is also compared with the measured data. The FEA computed results might differ from the measured values for one obvious reason: the 29th and 31st voltage harmonics in the measurements were produced by a generator supply unit. Fig. 5 compares the open-source, the commercial FEA results and the measured

current waveform and its FFT. Some of the harmonics is clearly present in the measured spectrum but negligible in the FEA computed waveforms as it originates from the supplying generator voltage. From the 17th to the 23rd harmonic, there is a significant difference between the amplitude of the measured and FEA computed waveforms, because the harmonics originate from the rotor slots. Furthermore, the higher amplitudes of these current harmonics (17th to the 23rd) in the simulation are a consequence of non-modelled skewing effect [28]. The FFT results for both software show torque ripple at the 6th harmonic resulting from the 5th and the 7th current linkage harmonics. The back-to-back test bench used in this study cannot be used to analyze the torque harmonics of the tested machine since the motor itself, the load machine and the test bench mechanics filter the harmonic torques, and thus, the torque transducer cannot observe them.

IV. Comparison of 2D, 2.5D and Measurements

Overall losses of a three-phase induction motor have been widely researched in literature [20]. The efficiency at the rated point of a small/medium-sized IM can be estimated with only one measurement at no-load using a method described in [29]. However, this method gives only the rated situation overall efficiency, and in this study, different frequencies are under investigation. Based on a 2D FEM, the iron losses are segregated in [28] into eddy, hysteresis and excess losses. The iron losses estimated analytically were less precise than calculated. An approach is introduced in [30] to estimate induction motor iron and copper losses by finite element analysis considering stator winding end effects, rotor end ring effects and the skewing of rotor bars. In this research, pure sinusoidal voltage was supplied to the real machine and to the finite element computation.

A. Measured iron losses

In this research, pure sinusoidal voltage was supplied without considering supply time harmonics. Time step FEA computations were performed to analyze losses at four different frequencies. Measured results were determined at four different frequencies of 50 Hz, 37.5 Hz, 25 Hz and 12.5 Hz with sinusoidal generator supply and constant *U/f* ratio, i.e the line-to-line voltages were 400 V, 300 V, 200 V and 100 V, respectively. The IEC [28] standard loss segregation method 2-1-1B was used to measure different motor loss components. Three tests were used to obtain the data for the loss segregation method. The stator and rotor Joule losses were determined from the rated load heat run test; the no-load voltage curve test was used to determine the mechanical losses and the iron losses; and the additional stray load losses were determined from the load curve test [28]. The measured values obtained using the IEC-segregation of losses method for losses at different supply frequencies are presented in Fig. 6.

B. Measured iron loss comparison with 2D FEA

Simulated outcomes from the open-source FEA are given in Table III. Computational FEA results showed that as the frequency increases, the total electrical losses in the machine increase as expected.

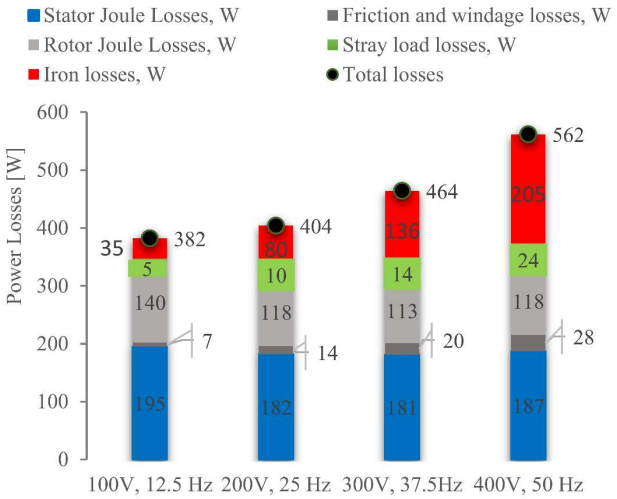

Fig. 6. Measured loss values at the rated load and 1.36 μΩ end-ring resistance for the 5 kW IM

TABLE III. Open-source computational results for different switching frequencies at the rated load of 32.5 Nm

f [Hz]	Parameters			
	P_{Fe} [W]	P_r [W]	P_s [W]	$P_{em,tot}$ [W]
12.5	34	130	155	319
25	81	124	153	358
37.5	138	122	149	409
50	207	125	151	483

The measured results differ from the ideal FEA computation since the supply unit generates some voltage harmonics which are not present in the FEA. Consequently, it can be expected that also the simulation results will deviate slightly from the measurement results. Analytical values for the iron losses at different frequencies and line-to-line voltage are compared with the FEA computed results in Fig. 7.

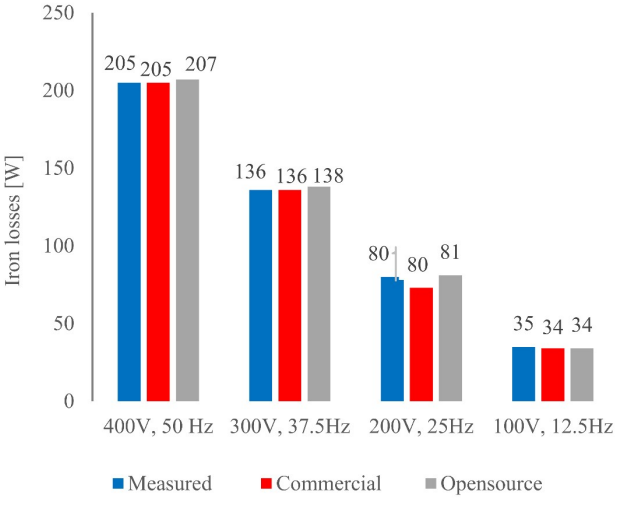

Fig. 7. Comparison of iron losses for measured and FEA computed values at 32.5 Nm load with end-ring resistance 1.36 μΩ for the 5 kW IM.

C. *Comparison between 2D, 2.5D FEA and measured losses*

In 2D, the waveforms have significant ripples because of the presence of the slotting effect. The slotting effect is usually reduced by skewing in a real machine [31]. Naturally, skewing is a 3D phenomenon and it can be precisely simulated only by using 3D FEM. However, it is possible to dissect the machine into several slices along the axis and solve the slices in 2D [14]. The proposed methodology in this research work highlights an option that is time-efficient and almost as accurate as 3D. The motor under consideration in this study has an 8.5-degrees skew along the rotor length of 160 mm. The slices are interconnected only through the electrical circuits, resulting in excellent scalability [8]. For 50 Hz, the measured rotor and stator joule losses are 118 W and 187 W respectively. The stator resistance value is set fixed for all the models. For the 2D case in Table IV, it can be seen that the rotor joule losses are 125 W and the stator joule losses are 151 W for the open-source FEM. However, for the 2.5D case, the rotor joule losses are reduced to 121 W, because the rotor losses are slip-related, with 0.023 as the slip value in each case. The stator joule losses reach 179 W, which is much closer to the measured value.

V. Analysis Time

One of the benefits of the open-source software platform is the freedom from selecting the number of cores. Thus, the calculation can be performed using as many cores as available. In the typical desktop configuration, four to eight cores are available and in laptops from two to four. It should be noted that the electromagnetics industry is still not making wide use of efficient parallel computation to solve complex design problems. The slow uptake of this technique might be a result of the higher complexity of parallel computing and, in some cases, the laborious and challenging task of parallelizing existing codes [30].

In electrical machines, both the rotor and stator usually have their own fixed meshes moving with respect to each other. The principal complication associated with the moving mesh approach is that the finite element meshes are generally non-matching across the shared interaction of bodies, and mortar boundary conditions are thus used [32]. Interface constraints in the mortar method are enforced over interacting non-conform domains in a variationally consistent way based on the Lagrange multiplier method. Additionally, the mortar method can preserve optimal convergence rates from the finite element methods, as long as appropriate mortar spaces are chosen [33]. However, for symmetrical bodies, conforming boundary conditions can be used. During the computation, not all nodes on conforming elements form part of a solution matrix as interstitial nodes are discarded. Due to this reduction in the number of nodes, the computational time can be reduced to some extent. From literature, it is seen that conforming elements have used three-quarters of the number of nodes to achieve the same accuracy as non-conforming elements [34]. In iron loss computation at 50 Hz supply, the commercial and open-source FEA time step size was set to 50 µs.

TABLE IV. Comparison of 2D and 2.5D Open-Source FEA Different Frequencies at Rated Load 32.5 Nm

Case	**Parameters**			
	P_{Fe} [W]	P_r [W]	P_s [W]	$P_{em,tot}$ [W]
2D	207	125	151	483
2.5D	206	121	179	506
Measured	205	118	187	510

Computational time comparison between mortar and conforming boundary conditions is shown for and the number of cores in Fig. 8. From the figure, it can be concluded that as the number of cores increases, the conforming boundary conditions for both 60,000 and 16,000 intervals require less computation time than the mortar boundary conditions. The relation of the computation time to the number of cores is not linear. When solving the problem using mortar boundary conditions, the computational time for 16,000 intervals declines by more than 50% when the number of cores is increased from 14 to 26. With conforming boundary conditions, computational time reduces from 238 hours to 19 hours with 26 cores for the former computational time and 3 cores for the latter with 60,000 time intervals. Computational time could be further reduced by using more parallelization.

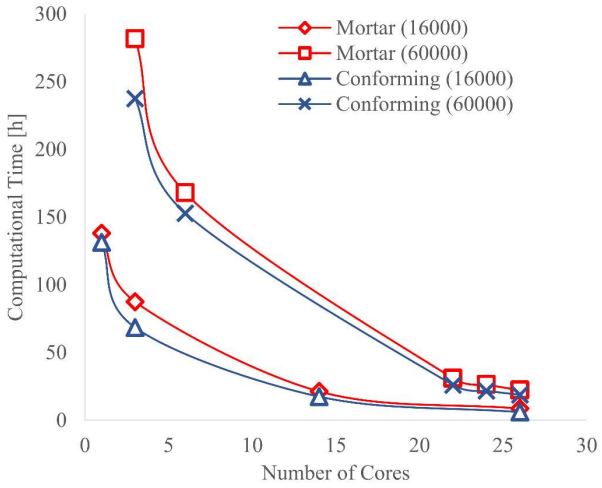

Fig. 8. Computational time against the number of cores for mortar and conforming boundary conditions.

Similar simulation is performed with commercial program: the same simulation time 0.8 s, mesh 120000 nodes, and 50 µs time-step. The simulation total time depends partly on the computer-unit which is processor Intel Xeon W-2135 3.7GHz, 6 cores and NVIDIA Quadro P2000, 5GB. The simulation took 33 hours, and this time is too long. Typically in FEA designing it is needed to vary the parameters, materials, and geometry and therefore the final solution requires a series of calculations. When one computation takes 33 hours, it will lead for long design/research time overall. In open-source using 6 cores took same time as commercial one to compute the results but, in open-source time efficiency can be further improved by accessing more cores.

VI. Discussion about the Sensitivity of Parameters

A. *Effect on losses by changing end winding inductance and end ring resistance*

Computation parameters are always theoretical and in the real machine some deviations occur because of manufacturing tolerances. E.g. air gap may not be exactly 0.5 mm as designed, and therefore authors were willing to make sensitivity analysis to see which parameters affect mostly the loss values. Variation in the dynamic performance of an induction motor is significantly dependent on the end winding inductance [35] and the rotor bar resistance. The resistance between the bars is part of the rotor resistance. Increasing rotor resistance increases the losses in the rotor circuit, and to overcome this loss, the stator current is increased. Nevertheless, the total electrical losses are mainly affected by changing the value of the rotor resistance [36].

In motor applications, the end winding inductance is generally considered to be a small or even negligible component of winding inductance [37] because its values are not very high, as it is far from the iron parts of the machine [21]. However, a significant percentage of the phase inductance may include end winding inductance, especially for motors with low length/diameter ratio or low-pitched winding. More accurate phase inductance calculation is required for such motors as it is a key parameter for designing a motor drive [37]. Fig. 9 presents a 3D graph illustrating how the end winding inductance and the ring resistance affect the iron losses of a 50 Hz induction machine when keeping the speed and conductivities constant. When the end winding inductance increases, the stator current THD is mitigated and the iron losses caused by the harmonics will be reduced. If the end ring resistance is reduced, the overall rotor equivalent resistance is reduced and, consequently, a smaller stator current is generated to produce the same amount of torque, which in turn leads to reduced iron losses.

B. *The Effect of varying air gap length on losses*

Changing the air gap length affects the machine losses. An efficient method to reduce the effects of the permeance harmonics, which are mainly caused by the stator slotting on the rotor surface, is to increase the air-gap length [37]. A longer air gap length will result in a higher magnetization current and stator copper losses [38]. In this study, the air gap length is varied to check its impact on the rated torque and stator current values, keeping all other parameters fixed.

Table V is illustrating the influence of the air gap length on torque, current and losses. The correlation revealed that the torque of the machine is reducing as the air gap is increasing and the current is showing the opposite trend. As the length of the air gap is increased, the reluctance of the magnetic circuit will increase, and the motor will create more magneto-motive force (MMF) to keep the required flux. To fulfil that extra MMF, the stator magnetizing current will increase, thus increasing the losses in the machine.

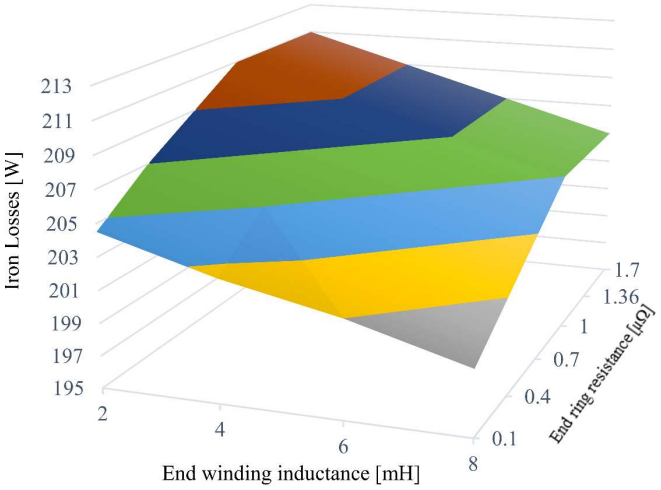

Fig. 9. 3D graph of parameters influencing iron losses.

TABLE V. Open-source FEA Computational Results by Varying Air Gap Length.

Air gap, mm	**Parameters**			
	I [A]	P_r [W]	P_s [W]	$P_{em,tot}$ [W]
0.3	8.9	134	140	479
0.4	9.15	126	148	480
0.5	9.3	125	151	482
0.6	10.89	118	209	536

C. *The Effect of stator tooth tip height on losses*

In this study, the stator tooth tip height is varied keeping all other parameters fixed to check the effect on the stator current values and stator joule losses. The stator tooth tip height considered in our model is 0.7 mm [15]. Table VI is showing the current RMS values for different slot heights, which are approximately the same for all the heights of stator slots.

Changing the stator tooth tip height from 0 to 2 mm has some impact on the stator current and loss values. From 0.4 to 2 mm, the current increases by 3.22% and the stator Joule loss values by 6.58 %. As this machine has a single layer winding and the 5th and 7th harmonics are strong, changing the tooth tip heights has a negligible effect at these harmonics. So, the current remains almost stable with varying tooth tip heights. The current has a comparatively high value for 0 mm, because of a decrease in the magnetization inductance or high Carter coefficient. The stator and rotor Joule losses will be greater at that particular height. Changing the stator slot opening might have a considerable effect on the stator current values. The THD% increases with increasing tooth tip height. Higher THD% indicates a less efficient motor, low power factor and higher losses.

TABLE VI. TOTAL HARMONIC DISTORTION FOR STATOR CURRENT BY VARYING TOOTH TIP HEIGHT

h_1	Parameters		
	I [A]	P_s [W]	THD%
0	10.1	181	14
0.4	9.35	155	12.2
0.7	9.40	156	12.3
0.8	9.43	157	12.5
1.2	9.51	160	12.6
1.6	9.59	163	13.5
2	9.62	164	17.1

VII. CONCLUSIONS

In 2D analysis of induction motors, parameters related to 3D phenomena are critical. The results are compared with measured data. 2D FEM analyses were performed for a 5 kW induction motor with commercial software Flux 2D and with an open-source software. The electromagnetic state of the machine remained the same throughout the whole analysis. FEA computed results from the open-source and commercial tools were compared with measured values. The experimentally determined value for the iron losses at 50 Hz is 205 W, while the open-source and commercial FEA computed values are 207 W and 205 W respectively.

At different frequencies and voltage values the open-source FEM showed acceptable and comparable results with the commercial FEA. Furthermore, the open-source error percentage was approximately 2% compared to the measured value. Adding skew in the 2.5D model has increased the accuracy of results for the motor electrical losses. Model parameters like the end winding inductance and the rotor bar resistance need to be accurate in machine design since they have an impact on iron losses. Additionally, by using 6 cores both FEA showed almost the same computational time. However, in open-source time can be significantly reduced by increasing the number of cores as they are easily accessed. It can be seen that the open-source software shows acceptable and faster results therefore, it is concluded that for 2D applications, it is possible to utilize the open-source platform in industrial-scale applications without incurring license fees. This study did not consider the skewing effect in the 2D models, which may have affected the accuracy of the results. A 3D model of the 5 kW induction motor will be studied in further work, along with further analysis of the skewing effect.

REFERENCES

[1] P. Råback, "Benefits of open source software for industry," CSC – IT Center for Science, 2013.

[2] Meeker, "Finite element method magnetics version 4.2 user'smanual," February 2009, http://www.femm.info/wiki/HomePage.

[3] R. Crozier and M. Mueller, "A new matlab and octave interface to a popular magnetics finite element code," *XXII International Conference on Electrical Machines (ICEM)*, Sept 2016, pp. 1251–1256.

[4] P. Dular and C. Geuzaine, "GetDP reference manual: the documentation for GetDP, a general environment for the treatment of discreteproblems," http://getdp.info, 2019

[5] A. Lehikoinen, T. Davidsson, A. Arkkio and A. Belahcen, "A High-Performance Open-Source Finite Element Analysis Library for Magnetics in MATLAB," *2018 XIII International Conference on Electrical Machines (ICEM)*, Alexandroupoli, 2018, pp. 486-492

[6] P. Bonneel, J. Le Besnerais, R. Pile and E. Devillers, "Pyleecan: An Open-Source Python Object-Oriented Software for the Multiphysic Design Optimization of Electrical Machines," *2018 XIII International Conference on Electrical Machines (ICEM)*, Alexandroupoli, 2018, pp. 948-954

[7] J. Keränen, J. Pippuri, M. Malinen, J. Ruokolainen, P. Råback, M. Lyly, and K. Tammi, "Efficient Parallel 3-D Computation of Electrical Machines With Elmer," *IEEE Transactions on Magnetics*, vol. 51, no. 3, pp. 1–4, 2015.

[8] J. Keränen, P. Ponomarev, J. Pippuri, P. Råback, M. Lyly and J. Westerlund, "Parallel performance of multi-slice finite-element modeling of skewed electrical machines," in *IEEE Transactions on Magnetics*, vol. 53, no. 6, pp. 1-4, June 2017, Art no. 7201204.

[9] D. Eggers, S. Steentjes and K. Hameyer, "Advanced iron-loss estimation for nonlinear material behavior," in *IEEE Transactions on Magnetics*, vol. 48, no. 11, pp. 3021-3024, Nov. 2012.

[10] K. Yamazaki, "An efficient procedure to calculate equivalent circuit parameter of induction motor using 3-D nonlinear time-stepping finite-element method," in *IEEE Transactions on Magnetics*, vol. 38, no. 2, pp. 1281-1284, March 2002

[11] S. Memon, D. Vallot, T. Zwinger, J. Åström, H. Neukirchen, M. Riedel, and M. Book, "Scientific workflows applied to the coupling of a continuum (Elmer v8.3) and a discrete element (HiDEM v1.0) ice dynamic model," Geoscientific Model Development, vol. 12, no. 7, pp. 3001–3015, 2019.

[12] U. Schuffenhauer, S. Miersch, N. Michalke, T. Schuhmann and A. Bárdos, "Modeling and practical investigation of the efficiency and operational behavior of induction machines with die-cast copper rotor," *2017 International Symposium on Electrical Machines (SME),* Naleczow, 2017, pp. 1-6.

[13] M. M. Stopa, M. A. Saldanha, A. A. Luiz, L. M. R. Baccarini and G. A. M. Lacerda, "A simple torque estimator for in-service efficiency determination of induction motors," *2017 IEEE Industry Applications Society Annual Meeting*, Cincinnati, OH, 2017, pp. 1-9.

[14] P. Ponomarev, "SEMTEC Report Elmer FEM - Induction Machine Tutorial," VTT Technical Research Centre of Finland LTD, DOI: 10.13140/RG.2.2.18599.75688, 2017

[15] M. Zaheer, P. Lindh, L. Aarniovuori, J. Pyrhönen, "Assessment of 5 kW Induction Motor Finite element computations with a Commercial and an Open-source software," in Proc. 2019 *ACEMP-OPTIM*, Istanbul, Turkey, pp. 114-119.

[16] R. De Weerdt, K. Hameyer and R. Belmans, "End ring inductance of a squirrel-cage induction motor using 2D and 3D finite element methods," *Conference Record of the 1995 IEEE Industry Applications Conference Thirtieth IAS Annual Meeting (IAS '95)*, Orlando, USA, Vol. 1, pp. 515-522, 1995.

[17] P. Lombard and F. Zidat, "Determining end ring resistance and inductance of squirrel cage for induction motor with 2D and 3D computations," *2016 XXII International Conference on Electrical Machines (ICEM)*, Lausanne, pp. 266-271, 2016.

[18] P. H. Trickey, "Induction motor resistance ring width," *Electrical Engineering*, vol. 55, no. 2, pp. 144–150, 1936.

[19] J. F. Fuller, E. F. Fuchs and D. J. Roesler, "Influence of harmonics on power distribution system protection," in *IEEE Transactions on Power Delivery*, Vol. 3, no. 2, pp. 549-557, April 1988.

[20] J. Langheim, "Modelling of rotorbars with skin effect for dynamic simulation of induction machines," *Conference Record of the IEEE Industry Applications Society Annual Meeting (IAS),* Vol.1 pp. 38 - 44, 1989.

[21] J. Pyrhönen, T. Jokinen, and Hrabovcová Valéria, *Design of rotating electrical machines*. Chichester, U.K.: J. Wiley & Sons, 2014.

[22] A. Belahcen, P. Rasilo and A. Arkkio, "Segregation of iron losses from rotational field measurements and application to electrical machine," in *IEEE Transactions on Magnetics*, vol. 50, no. 2, pp. 893-896, Feb. 2014, Art no. 7022104.

[23] A. N. Abdul Saheb and A. M. Ali, "Estimation of copper and iron losses in a three-phase induction motor using finite element analysis," *2018 2nd International Conference for Engineering, Technology and Sciences of Al-Kitab (ICETS)*, Karkuk, Iraq, 2018, pp. 6-10.

[24] P. A. Hargreaves, B. C. Mecrow and R. Hall, "Calculation of Iron Loss in Electrical Generators Using Finite-Element Analysis," in *IEEE*

Transactions on Industry Applications, vol. 48, no. 5, pp. 1460-1466, Sept.-Oct. 2012.

[25] "Flux™ 2018 Release Notes," Altair Engineering, Inc., 2018.

[26] M. Lyly, "ElmerGUI manual," CSC – IT Center for Science, online http://www.nic.funet.fi, 2015.

[27] J. Kortelainen, "Meshing Tools for Open Source CFD – A Practical Point of View," *VTT Technical Research Centre of Finland LTD*, www.vttresearch.com, 2009.

[28] P. Lindh, L. Aarniovuori, H. Kärkkäinen, M. Niemelä and J. Pyrhönen, "IM Loss Evaluation Using FEA and Measurements," *2018 XIII International Conference on Electrical Machines (ICEM),* Alexandroupoli, 2018, pp. 1220-1226.

[29] M. Al-Badri, P. Pillay and P. Angers, "Simple and accurate algorithm for small- and medium-sized three-phase IM efficiency estimation based on no-load tests," *IEEE Transactions on Industrial Appl*., Vol. 54, n. 6, pp. 5812–5821, Nov/Dec. 2018

[30] E. Takala, E. Yurtesen, J. Westerholm, J. Ruokolainen and P. Råback, "Parallel simulations of inductive components with Elmer finite-element software in cluster environments," *Electromagnetics*, vol. 36, no. 3, pp. 167-185, 2016.

[31] P. Ponomarev, L. Aarniovuori and J. Keränen, "Selection of optimal slice count for multi-slice analysis of skewed induction motors," *IECON 2017 - 43rd Annual Conference of the IEEE Industrial Electronics Society*, Beijing, 2017, pp. 2149-2153.

[32] J. Ruokolainen, M. Malinen, P. Råback, T. Zwinger, A. Pursula and M. Byckling, "ElmerSolver Manual," www.nic.funet.fi, 2019.

[33] O. Lloberas-Valls, M. Cafiero, J. Cante, A. Ferrer and J. Oliver, "The domain interface method in non-conforming domain decomposition multifield problems," *Computational Mechanics*, vol. 59, no. 4, pp. 579-610, 2016.

[34] C. Brebbia and G. Gipson, Boundary Elements XIII. Springer Netherlands, pp. 935-938.

[35] J. H. J. Potgieter and M. J. Kamper, "Calculation Methods and Effects of End-Winding Inductance and Permanent-Magnet End Flux on Performance Prediction of Nonoverlap Winding Permanent-Magnet Machines," in *IEEE Transactions on Industry Applications*, vol. 50, no. 4, pp. 2458-2466, July-Aug. 2014.

[36] A. Hanif, S. M. N. Ali, Q. Ahmed, A. I. Bhatti, G. Yin and M. H. Jaffery, "Effect of variation in rotor resistance on the dynamic performance of induction motor," *2016 35th Chinese Control Conference (CCC)*, Chengdu, 2016, pp. 9524-9529.

[37] M. Hsieh, Y. Hsu, D. G. Dorrell and K. Hu, "Investigation on end winding inductance in motor stator windings," in *IEEE Transactions on Magnetics*, vol. 43, no. 6, pp. 2513-2515, June 2007.

[38] M. Valtonen, A. Parviainen and J. Pyrhönen, "Influence of the air-gap length to the performance of an axial-flux induction motor," *2008 18th International Conference on Electrical Machines*, Vilamoura, 2008, pp. 1-5.

Minhaj Zaheer born in Khanewal, Pakistan in 1988 received the B.Eng. Degree in Engineering Science from GIK Institute of Science and Technology in year 2011. M.Sc. degree in Computational Engineering from Lappeenranta University of Technology (LUT), Finland in 2016. Currently, enrolled as PhD candidate in Electrical Engineering at Lappeenranta University of Technology (LUT), Lappeenranta, Finland. Main interests are modeling and simulation of 2D and 3D electric drives.

Pia Lindh (M'04, SM'17) born in Helsinki in 1969, received her M.Sc. degree in energy technology in 1998 and her D.Sc. degree in electrical engineering (Technology) in 2004 from Lappeenranta University of Technology (LUT), Lappeenranta, Finland. She is currently serving as an associate professor at the Department of Electrical Engineering in LUT Energy, Lappeenranta, where she is engaged in teaching and research of electric motors and electric drives.

Lassi Aarniovuori (M'15, SM'19) was born in Jyväskylä, Finland, in 1979. He received M.Sc. and D.Sc. degrees in electrical engineering from Lappeenranta University of Technology (LUT), Lappeenranta, Finland, in 2005 and 2010, respectively. Dr. Aarniovuori was a Marie Curie Fellow with the School of Engineering and Applied Science, Aston University, UK during 2017-2019. Currently, he is serving as an Adjunct Professor of Electric Motors and Drives at LUT. His current research interests include the field of electric motor drives, especially wide band-gap power switches, modulation methods, simulation of electric drives, efficiency measurements, and calorimetric measurement systems.

Juha Pyrhönen (M'06, SM'18) born in 1957 in Kuusankoski, Finland, received the Doctor of Science (D.Sc.) degree in Electrical Engineering from Lappeenranta University of Technology (LUT), Finland in 1991. He became Professor of Electrical Machines and Drives in 1997 at LUT. He is engaged in research and development of electric motors and power-electronic-controlled drives. Prof. Pyrhönen has wide experience in the research and development of special electric drives for distributed power production, traction drives and high-speed applications. Permanent magnet materials and applying them in machines have an important role in his research. Currently, he is also researching new carbon-based materials for electrical machines.